ORIGINAL ARTICLE

Seascape genomics identify adaptive barriers correlated to tidal amplitude in the shore crab *Carcinus maenas*

Marlene Jahnke[1] | **Per-Olav Moknes**[2] | **Alan Le Moan**[1] | **Gerrit A. Martens**[1] | **Per R. Jonsson**[1]

[1]Department of Marine Sciences, Tjärnö Marine Laboratory, University of Gothenburg, Strömstad, Sweden

[2]Department of Marine Science, University of Gothenburg, Gothenburg, Sweden

Correspondence
Marlene Jahnke, Department of Marine Sciences, Tjärnö Marine Laboratory, University of Gothenburg, Strömstad, Sweden.
Email: marlene.jahnke@gu.se

Present address
Gerrit A. Martens, Institute of Zoology, University of Hamburg, Hamburg, Germany.

Abstract

Most marine invertebrates disperse during a planktonic larval stage that may drift for weeks with ocean currents. A challenge for larvae of coastal species is to return to coastal nursery habitats. Shore crab (*Carcinus maenas* L.) larvae are known to show tidal rhythmicity in vertical migration in tidal areas and circadian rhythmicity in microtidal areas, which seems to increase successful coastal settlement. We studied genome-wide differentiation based on 24,000 single nucleotide polymorphisms of 12 native populations of shore crab sampled from a large tidal amplitude gradient from macrotidal (~8 m) to microtidal (~0.2 m). Dispersal and recruitment success of larvae was assessed with a Lagrangian biophysical model, which showed a strong effect of larval behaviour on long-term connectivity, and dispersal barriers that partly coincided with different tidal environments. The genetic population structure showed a subdivision of the samples into three clusters, which represent micro-, meso- and macrotidal areas. The genetic differentiation was mostly driven by 0.5% outlier loci, which showed strong allelic clines located at the limits between the three tidal areas. Demographic modelling suggested that the two genetic barriers have different origins. Differential gene expression of two clock genes (*cyc* and *pdp1*) further highlighted phenotypic differences among genetic clusters that are potentially linked to the differences in larval behaviour. Taken together, our seascape genomic study suggests that tidal regime acts as a strong selection force on shore crab population structure, consistent with larval behaviour affecting dispersal and recruitment success.

KEYWORDS
behaviour, biophysical modelling, *Carcinus maenas*, gene expression, gene flow, seascape

1 | INTRODUCTION

Local adaptation is the fine-tuning of populations to their local environment via natural selection (Savolainen et al., 2013). Selective forces driven by environmental differences result in locally adapted populations with resident genotypes having higher fitness in their native habitat (Kawecki & Ebert, 2004). However, the diversifying effects of selection will be opposed by the homogenizing effect of gene flow (Nosil, 2009). In the marine environment, where seascape genetics and genomics have only recently helped "to navigate the currents" (Riginos et al., 2016), microgeographical adaptation (adaptation at a spatial scale smaller than dispersal; *sensu* Richardson et al.,

2014) seems surprisingly common despite the high gene flow potential of many marine species (Sanford & Kelly, 2011). For instance, locally adapted populations have been described in microalgae and fish which have planktonic propagules that disperse passively for weeks in the water column (Barth et al., 2019; Sjöqvist et al., 2015). One of the potential processes driving this differentiation is purifying selection, which acts in each generation following dispersal. Purifying selection, also referred to as "phenotype–environment mismatch" (Marshall et al., 2010), can maintain allelic differences despite high gene flow. Further, the presence of genomic structural variation reducing recombination between co-adapted alleles might favour the maintenance of local adaptation despite high gene flow (Barth et al., 2019; Cayuela et al., 2020; Le Moan et al., 2021). Alternatively, secondary contact after past isolation might facilitate the initial increase in frequency of adaptive variation despite gene flow (Ravinet et al., 2017; Rougemont et al., 2017). Finally, plasticity in gene expression is also an important factor in local adaptation (Kenkel & Matz, 2016). Phenotypic plasticity can provide a short-term buffer during longer-term genetic adaptation (Munday et al., 2013). The flip side of plasticity is that selection may be too weak to winnow less fit individuals, and therefore no gradual adaptation to a changing environment that may finally surpass the range of plasticity (Ho & Zhang, 2018). In contrast to these processes driven by selection, there also may be bias in gene flow when genetic variation leads to intraspecific variation in behaviour linked to dispersal, generating gene flow that is nonrandom with respect to individual variation (Edelaar & Bolnick, 2012). Any nonrandom gene flow can lead to local adaptation or it can lead to patterns that resemble local adaptation, but do not involve any fitness differences and/or evolutionary processes (i.e., natural selection). Looking at the question from the other side of the coin, there is also the issue "when is dispersal for dispersal?" (Burgess et al., 2016). The relationship between dispersal and fitness may not be as simple and direct as often assumed, and in fact in the marine environment dispersal has also often been viewed as an incidental by-product of traits selected for other functions (Bonhomme & Planes, 2000).

The European shore crab (*Carcinus maenas* L.) is particularly well suited for assessments of the relationship between dispersal and adaptation, because of its particular life history and its long history as an object of scientific study including dispersal. The shore crab is also of global concern since it has successfully invaded several continents (Grosholz & Ruiz, 1996) and poses an ecological threat in many coastal areas (e.g., Pickering et al., 2017). Shore crabs have a lifespan of 3–5 years and a generation time of 2–3 years (Crothers, 1967). As adults they are mostly solitary and adult dispersal is limited to tens of kilometres. Larval dispersal is, however, possible—at least potentially—over large geographical distance as the larvae drift for 4–10 weeks in the water column depending on the water temperature (Dawirs, 1985; Mohamedeen & Hartnoll, 1989; Yamada et al., 2015). The population genetics/genomics of *C. maenas* are relatively well studied, but mostly focus has been on parts of the introduced range along the west Atlantic coast (Darling et al., 2014; Jeffery, DiBacco, Wringe, et al., 2017; Jeffery, DiBacco, Van Wyngaarden,

et al., 2017; Roman, 2006; Tepolt & Palumbi, 2015). Interestingly, shore crab larvae in the native range show a cline in larval behaviour (vertical migration) along a gradient in tidal influence from macrotidal (>4-m tidal range) areas along the British Isles to microtidal areas (<1-m tidal range) in the Skagerrak area of the eastern North Sea (Moksnes et al., 2014; Queiroga et al., 2002). In meso- and macrotidal areas, shore crab larvae display an inherited endogenous vertical migration rhythm (Duchêne & Queiroga, 2001; Zeng & Naylor, 1996c), which when synchronized with local tides is believed to facilitate cross-shelf transport and recruitment success (Queiroga, 1998; Zeng & Naylor, 1996a). Importantly, this tidal rhythmic behaviour was even displayed by newly hatched larvae from mothers that had been kept in a constant environment for months, but originally came from a macrotidal area (Zeng & Naylor, 1996c), suggesting that this behaviour is heritable (Zeng & Naylor, 1996b). This endogenous tidal rhythm is not present in larvae from microtidal areas, where instead larvae show an exogenous circadian rhythm with migration to deeper waters during the day, possibly reducing predation (Moksnes et al., 2003, 2014; Queiroga et al., 2002). As the velocity and direction of coastal ocean currents often vary with depth, the vertical position of pelagic larvae may critically affect their dispersal (Corell et al., 2012; Moksnes et al., 2014), and this adaptation in behaviour is therefore hypothesized to be an optimal strategy between avoiding inshore stranding, enhancing offshore dispersal of the larvae, predator avoidance and larval recruitment to shallow nursery areas (Moksnes et al., 2014).

Here we hypothesize that tidal regime exerts a strong selection pressure for different vertical migration behaviours of *C. maenas* larvae, which is probably modulated by gene expression differences in clock genes. We further hypothesize that larvae with the "wrong" tidal behaviour will have reduced recruitment success, which restricts along-coast dispersal resulting in genetic population differentiation in an isolation-by-distance manner and between geographical areas with different tidal regimes. To address these hypotheses, we sampled 12 populations along a tidal gradient in the North Sea from macro- to microtidal conditions, and used a combination of approaches to examine (i) dispersal distances and connectivity of the shore crab metapopulation based on biophysical modelling, (ii) historical and contemporary patterns of gene flow inferred from ~24,000 single nucleotide polymorphisms (SNPs) generated with 2b-RAD sequencing and a demographic model, and (iii) gene expression differences of putative clock genes.

2 | MATERIAL AND METHODS

2.1 | Sampling

Guided by observed behavioural differences between crab larvae of macro- and microtidal environments (Moksnes et al., 2014) and a previous genetic assessment of *Carcinus maenas* in central Europe (Roman & Palumbi, 2004), we carried out sampling at 12 sites (Figure 1) in September and October 2017 along a tidal cline from

macrotidal (>4 m) in Wales (Bangor: 8.6 m) and the English Channel (Dunkirk: 7.0 m) to microtidal (<2 m) in the Kattegat (Odense: 0.22 m, www.tide-forecast.com, Table 1). One site in the mesotidal area, Hvide Sand, is experiencing a low tidal amplitude due to an artificial barrier (Table 1). The sites span a geographical range of
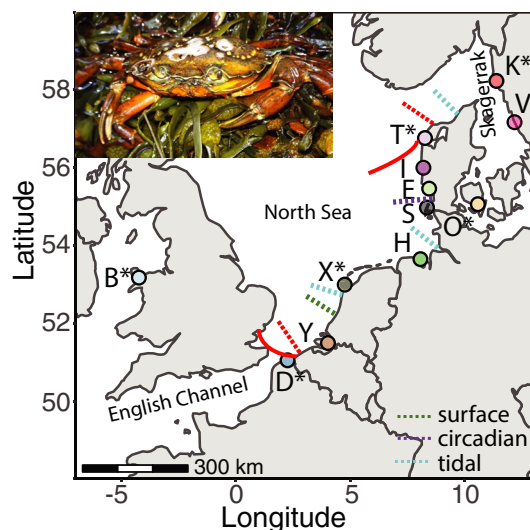
FIGURE 1 Map of *Carcinus maenas* sampling locations in the North Sea. Site acronyms with a star have been included in the gene expression analysis. Acronyms are as follows: O, Odense; V, Varberg; K, Kristineberg; T, Tyboron; I, Hvide Sand; E, Esbjerg; S, Sylt; H, Hooksiel; X, Texel; Y, Yerseke; D, Dunkirk; B, Bangor. Red lines indicate distinctions between micro- (<2 m) in the Skagerrak and Kattegat, meso- (2–4 m) in the Wadden sea and macrotidal (>4 m) in the English channel according to Jänicke et al. (2020). Red dotted lines indicate "adaptive barriers" as identified in Figure 4. Turquoise, purple and green dotted lines indicate barriers to dispersal identified from the multigenerational stepping-stone biophysical modelling for the three behaviours: surface dispersal (green barrier), circadian behaviour (purple) and tidal behaviour (turquoise)

~2000 km sea-distance between Bangor and Odense. Sampling was performed at similar geographical distances among sites and males and females were collected in equal proportions at each site. For genotyping, 10 males and 10 females were assessed at each of the 12 sites, whereas for gene expression analyses, four males and four females were used from only six of the sites, including the full tidal gradient (Figure 1). The crabs were dredged (Bangor, Yerseke, Esbjerg, Hvide Sand and Sylt), caught in fyke nets (Texel) or caught in baited traps (Dunkirk, Hooksiel, Tyboron, Kristineberg, Varberg and Odense). For genotyping, one leg from each living individual was removed, transferred to ethanol and immediately stored at −20°C. For gene expression analyses, leg muscle tissue was directly transferred to RNAlater (Ambion, Life Technologies), kept overnight at 4°C, transported at −20°C and finally stored at −80°C until RNA extraction. Crabs were released at the site of capture when possible. We additionally sampled shore crab megalopae at the Kristineberg site (58.259°N, 11.450°E; Figure 1) in the morning of August 22, 2019 with a plankton net (500 μm) at 15–20 m depth to verify candidate gene expression in larvae.

2.2 | Biophysical model of multigenerational larval dispersal

We used a biophysical model to explore the effects of different larval behaviour strategies on multigenerational dispersal distance and to identify possible barriers along the tidal gradient from the English Channel to the Kattegat area. Dispersal trajectories were simulated with a Lagrangian particle-tracking model (TRACMASS, Vries and Döös, 2001) driven off-line with flow fields (3-hr resolution) from an ocean circulation model (NEMO-Nordic, Hordoir et al., 2019). The model has a horizontal spatial resolution of 3.7 km, 84 vertical levels, a free surface and allows the grid boxes to stretch and shrink vertically to model the tides without generating empty grid cells at

TABLE 1 Information on sampling sites of *Carcinus maenas* included in the analysis and sorted along a geographical line from the Kattegat to the Irish Sea

Site	Acronym	Latitude (°N)	Longitude (°E)	Sampling date and time for gene expression (for those sampled)	Tidal range (m)
Odense	O	54.9849	10.6329	Afternoon October 9, 2017	0.22
Varberg	V	57.1108	12.2392		0.16
Kristineberg	K	58.2499	11.4464	Morning October 6, 2017	0.34
Thyborøn	T	56.7062	8.2209	Morning September 30, 2017	2.14
Hvide Sand	I	56.0044	8.1296		1.15
Esbjerg	E	55.4896	8.4107		2.15
Sylt	S	55.0404	8.4591		2.1
Hooksiel	H	53.6436	8.0839		3.35
Texel	X	52.9968	4.7766	Midday September 26, 2017	2.65
Yerseke	Y	51.488	4.0578		3.24
Dunkirk	D	51.0464	2.3744	Morning September 25, 2017	7.03
Bangor	B	53.2265	−4.1589	Morning October 23, 2017	8.56

low tide. To mimic larval vertical behaviour, the vertical position of the trajectories was locked at predetermined depths, changing with tidal, circadian and ontogenetic periods (Moksnes et al., 2014).

We included three different larval behaviours in this modelling effort (tidal, circadian and surface). Particles, simulating larvae, were released from 1360 model grid cells spanning the tidal cline from the English Channel to the Kattegat. Grid cells adjacent to land were assumed to include shallow-water habitat typical for adult shore crab and suitable for spawning and settling; a few offshore grid cells, with a mean depth ≤6 m, were also included. Release of a total of 600,000 particles occurred at the end of June to coincide with a peak recruitment period of juvenile crabs in July and August in Northern Europe (Breteler-Klein, 1976; Moksnes, 1999). The release was repeated for three years (1989, 1996 and 2003), representing two opposite extremes and one neutral year in the North Atlantic oscillation cycle (Hurrell & Deser, 2010). The number of release time points between and within years was a compromise in the modelling effort. In a previous study of dispersal of *C. maenas* larvae (Moksnes et al., 2014), we showed that dispersal metrics (distance to shore after dispersal and recruitment success) mainly depended on larval behaviour and the geographical location of release. Release time played a minor role, with variation between years more important than between months during the reproductive season. In this study of the full connectivity between shallow areas we therefore only included interannual variation. The dispersal simulations included a fixed pelagic larval duration of 40 days, consisting of 25 days of zoeal stages and 15 days of the megalopal phase (Mohamedeen & Hartnoll, 1989). Trajectories of the tidal behaviour shifted depths according to the selective tidal stream transport hypothesis (Queiroga et al., 1994), and were located at the surface (0.3 m depth) during ebbing tides and at 20 m depth during flooding tides for the first 25 days. For the last 15 days of the larval phase, the trajectories were given the opposite vertical migration pattern. The tidal migration was synchronized with the principal lunar semidiurnal tidal constituent (M2; 12.42-hr period), which is the dominant tidal signal in the North Sea (Hill, 1995). The tidal behaviour further changed its rhythm to be in phase with the local tide. Trajectories for the circadian behaviour shifted depth according to the sea-breeze hypothesis (Shanks, 1995), and were located at the surface (0.3 m depth) during night and twilight conditions and at 20 m depth at daylight hours for the first 25 days with the opposite pattern for the last 15 days. Particles that dispersed according to the surface behaviour drifted at 0.3 m depth during the entire larval duration of 40 days.

From these trajectories the dispersal probabilities between all 1360 grid cells were calculated and summarized in a connectivity matrix (Jonsson et al., 2020). We also calculated the multigeneration connectivity where stepping-stone dispersal is allowed over many single-generation dispersal events, and summed over all possible dispersal routes (White et al., 2010). Such multigeneration connectivity may be used to infer the long-term connectivity between populations (e.g., exploring barriers to gene flow) (Jahnke et al., 2018). Multigeneration connectivity was calculated by multiplication of the connectivity matrix across 64 generations, which seemed

an appropriate time span to potentially disperse from the English Channel to the Kattegat (~1200 km).

2.3 | DNA extraction and 2b-RAD library preparation

DNA was extracted with RNAse treatment, and four out of 20 individuals from each locality were also used as technical replicates (i.e., replicated extraction, library preparation and sequencing). DNA extraction was followed by an ethanol/isopropanol precipitation. DNA quantity and quality were assessed using a Qubit ds DNA BR or HS AssayKit (Invitrogen–ThermoFisher Scientific) and on a 1% agarose gel.

2b-RAD libraries (Wang et al., 2012) were prepared following a laboratory protocol available at https://github.com/z0on/2bRAD_denovo, using the restriction enzyme *Bcg*I. Libraries were individually barcoded, and fragment selection was performed by excising the amplicon band from an agarose gel. Gel fragments were cleaned using a MinElute Gel Extraction Cleaning Kit (Qiagen) and pooled equimolarly (as assessed by the Qubit ds DNA HS AssayKit) into population sets of 24 individuals (20 individuals plus four technical replicates) per sequencing lane. In total, 240 crab samples from 12 sites and 48 technical replicates were sequenced in 12 libraries on the Illumina HiSeq2500 platform, generating 50-bp single-end sequences, at the Science for Life Laboratory (SciLifeLab)—Genomics, SNP&SEQ Technology Platform in Uppsala University, Sweden.

2.4 | Bioinformatics pipeline

Bioinformatics were performed using the computer cluster "Albiorix" at the University of Gothenburg, Sweden. The analysis followed a modified *de novo* pipeline available at https://github.com/z0on/2bRAD_denovo. Reads were "demultiplexed" based on barcodes. Restriction sites were trimmed off, followed by quality filtering using the fastx-toolkit (stating that 100% of bases should have a quality score of at least 20, which means a 1% error rate). After trimming and quality filtering, a total of 1,352,415,682 reads were retained across the 12 libraries. Individual trimmed fastq files were merged to collect tags found in at least two individuals with a minimum depth of five for genotyping. Reads that had more than seven observations but lacked reverse complement reads were removed. Tags were then clustered with cd-hit (Li & Godzik, 2006) allowing for up to three mismatches, followed by the creation of a "reads-derived reference" based on 30 fake chromosomes. Individual trimmed fasta files were mapped back to the references. Then, genotyping was performed using The Genome Analysis Tookit version 3.1-1 (GATK) (McKenna et al., 2010). A first round of putative variants was generated using GATK's UnifiedGenotyper, followed by base quality score recalibration (BQSR/BaseRecalibrator and PrintReads) based on a high-confidence (>75th quality percentile) SNP set. The realigned and recalibrated reads were used to generate a second round using

UnifiedGenotyper. We then used the variant quality score recalibration (VQSR) step, to generate an adaptive error model using the SNPs that were reproducibly genotyped across the technical replicates. When applying the recalibration we chose the tranche with 95% truth sensitivity, which had a Ti/Tv ratio of 1.784, to call all SNPs from the overall data set. The final filtration step was performed in VCFTOOLS (Danecek et al., 2011) to remove under-sequenced samples (set to fewer than 95 000 sites, which removed three individuals) and to select biallelic loci genotyped in at least 90% of individuals, and with a maximum heterozygosity of 50%. This resulted in a final data set of 81,389 loci for 240 unique individuals.

2.5 | Population genetic analyses

2.5.1 | Population structure

Population genetic analyses were performed on the Rackham cluster of the Swedish National Infrastructure for computing (SNIC). The final data set was thinned in order to keep one SNP per RAD locus with maximal allele frequency (script thinner.pl with criterion = maxAF, https://github.com/z0on/2bRAD_denovo), resulting in 24,273 loci. Individual genetic variation was visualized by a principal component analysis (PCA) using the R package adegenet (Jombart, 2008). BAYESCAN (Foll, 2012) was used to identify putative loci under selection with prior odds set to 100, using a relaxed threshold of $q = 0.5$ and a stringent threshold at $q = 0.00011$ (see Figure S1 for BAYESCAN plot). In an attempt to annotate the 128 outlier loci, we first blasted the short 36-bp 2bRAD fragments against the *C. maenas* Transcriptome Shotgun Assembly (TSA), and then used the *blastn* algorithm to query the longer-sequence TSA hits. Sea distances without crossing land were calculated in the R package marmap (Pante & Simon-Bouhet, 2013). Pairwise Weir and Cockerham's F_{ST} and linkage disequilibrium were calculated among sites using VCFTOOLS (Danecek et al., 2011) for outlier and putatively neutral loci. We explored the variation of allele frequency across geographical distance for the outlier loci using cline model fitting with the R package HZAR (Derryberry et al., 2014). For each outlier, we calculated the slope of the cline by calculating the differences in allele frequency estimated by the model on each side of the cline, and dividing this difference by the cline width. The slope values were then represented against the position of the cline centres estimated from the model using the R package ggplot2 (Wickham, 2016). We tested for isolation-by-distance (IBD) between the pairwise F_{ST} (of all loci, neutral loci and outlier loci) and sea distance as well as dispersal probability obtained with the biophysical model using Mantel tests with the R package ncf (Bjornstad, 2009) with 100,000 replicates. For visualization, connectivity networks based on F_{ST} (neutral and outlier loci) and biophysical dispersal probability (three behaviours: surface drifting, migrating in rhythm with day/night or in rhythm with the tides) were drawn using the R packages igraph (Csardi & Nepusz, 2006) and popgraph (Dyer, 2014). All edges are shown for estimated dispersal probabilities, while for F_{ST} several cut-offs were explored, and those

that resulted in still connected networks are shown (similar to the percolation threshold). For IBD and network analyses, we removed the site Bangor from the analysis, as it lies beyond the oceanographic model domain.

2.5.2 | Demographic history

In addition to the contemporary connectivity patterns, we evaluated historical population connectivity using the software MOMENTS (Jouganous et al., 2017). Inferences were conducted between two pairs of sampling sites representative of the main genetic clusters: Dunkirk (D, macrotidal) vs. Sylt (S, mesotidal), and Sylt vs. Kristineberg (K, microtidal, Figure 1). The data were filtered to keep one random SNP per RAD tag with a minor allelic count of at least two among the three geographical sites. The folded version of the Site-Frequency-Spectrum (SFS) was used to compare contrasted models of demographic history. Four basic models of population splits were compared: Strict Isolation (SI), Isolation with Migration (IM), Ancestral Migration (AM) and Secondary Contact (SC). These models were further tuned to include changing effective population sizes either in the ancestral population (model "ac" for ancient change) or, after the split, in one of the daughter populations (model "rc" for recent change). In addition, models of heterogeneous effective population size (model "2N") and heterogeneous migration rate (model 2 m in the model with gene flow: IM, SC, AM) resulting from the effect of selection at linked sites and intrinsic barriers to gene flow, were included (Table S1). The models were adjusted to the data following the three-step optimization procedure developed by Portik et al. (2017) adapted to the software MOMENTS by Momigliano et al. (2021). The fit of each model was replicated 10 times to control for parameter convergence. In total, the fits of 44 demographic scenarios were compared using Akaike's information criterion (AIC) value, the Δ_{AIC} ($AIC_{best}-AIC_i$), and the weighted AIC (see Rougeux et al., 2017). The estimates of divergence time were converted into years following Rougeux et al. (2017) using a mutation rate of 1×10^{-8} per generation, and a generation time of 3 years (Crothers, 1967).

2.6 | Candidate gene approach for gene expression analyses

Using a candidate gene approach, we also looked at gene expression differences of insect candidate clock genes, probably involved in the differing crab larvae behaviour between tidal and atidal sites. We extracted RNA from ~100 mg of muscle tissue from eight individuals (four males and four females) each at six sites with the RiboPure kit (Life Technologies) according to the manufacturer's instructions. For the extraction of larval RNA, 50 megalopae were combined. We used the high-capacity cDNA Reverse transcription kit (Applied Biosystems) with 500 ng of RNA as input material to synthesize cDNA according to the manufacturer's instructions.

Searches for *C. maenas* clock genes were conducted using a protocol previously applied to discover circadian genes/proteins in other crustaceans (Biscontin et al., 2017; Christie et al., 2018). First, *tblastn* (http://blast.ncbi.nlm.nih.gov/Blast.cgi) was used to search through the "Transcriptome Shotgun Assembly (TSA)" database of "*Carcinus* (taxid: 6758)." Known circadian proteins, primarily those from the fruit fly *Drosophila melanogaster*, were used as query sequences in *tblastn* (15 circadian proteins from *D. melanogaster* and two circadian proteins from *Danaus plexippus*). In addition, we selected four genes that have been suggested to be tidally linked in the limpet *Cellana rota* (Schnytzer et al., 2018; see Table S2). Primers for gene expression analyses with quantitative real-time polymerase chain reaction (qPCR) were designed with PRIMER3 (http://primer3.ut. ee). Design conditions included primer length (18–23 bp), T_m (~60°C), GC content (≥50%) and a product size of 150–200 bp. In qPCRs we used the Fast Sybr Green Master mix (Applied Biosystems) as per the manufacturer's instructions and a thermal profile of 95°C for 20 s, followed by 40 cycles of 95°C for 1 s and 60°C for 20 s. All qPCRs were conducted in technical triplicates and each assay included three no-template negative controls (NTCs). Primer sequences, percentage efficiencies (*E*) and regression coefficients (R^2) of the candidate and reference genes are reported in Table S3. Three reference genes, elongation factor (*cm-ef2*), elongation factor-1 (*camelf1a*) and Ubiquitin-conjugating enzyme E2 L3 (*camubce2*) (Abuhagr et al., 2014; Alexander et al., 2018), were selected to normalize the transcription profiles of the 21 candidate genes for each sample. STEPONE software version 2.3 was used to calculate raw threshold cycle (Ct) values and to analyse the endogenous control genes. To analyse differences in gene expression among samples (*n* = 48) and sites (*n* = 6), the sample maximization method according to Hellemans et al. (2007) was established. The significance of gene expression differences among populations and clusters was tested with the REST 2009 software (Pfaffl et al., 2002), followed by Benjamini–Hochberg false discovery rate corrections (Benjamini & Hochberg, 1995). Linear mixed models (LMMs) were performed using the function "*lmer*" in the lme4 package in R (Bates et al., 2014), with tidal gradient (scored 1–6), latitude, sampling date (days after equinox) and sampling time (morning, midday or afternoon) as fixed effects that were fitted to the dependent variable (normalized relative quantity [NRQ] of each of the 21 candidate genes separately). As a random effect, we had intercepts and random slopes for sex at each site (12 levels). Visual inspection of residual plots did not reveal any obvious deviations from homoscedasticity or normality. By examining backward reduced random-effect tables generated with the package "*lmerTest*" (Kuznetsova et al., 2017), we found that latitude and sex at each site were not a significant factor for gene expression differences in any of the candidate genes (Table S4). These two factors were removed for the final full model, which used tidal gradient, sampling time and sampling date as fixed factors using "*lm*" of the stats package. A top-down approach was then used for each candidate gene separately to compare the fit of the fully fitted model to (i) a model without the tidal gradient, (ii) without date and (iii) without sampling time, with analysis of variance (ANOVA). This analysis allowed us to identify candidate genes that exhibited a significant transcriptional response to the three factors that might affect circadian clock gene expression. To assess trends of overall gene expression, we performed a PCA to reduce the data based on all candidate genes, all clock genes, core clock genes, clock-associated genes and putative tidal cyclers. Finally, we used the PC1s as input for *lm* for overall changes in gene expression of each gene group. A heatmap was created with the gplots R package (Warnes et al., 2009) using population NRQ values standardized to the microtidal population from Odense and the genes *cyc* and *pdp1*.

3 | RESULTS

3.1 | Biophysical model of multigenerational stepping stone larval dispersal

The biophysical model of multigeneration, stepping-stone dispersal predicted some potential barriers to gene flow in the North Sea–Skagerrak–Kattegat transition. The number, strength and geographical position of potential barriers depended on the simulated vertical larval behaviour (Figure 1; Figure S2). Larvae drifting in surface water during the full 40-day period showed the highest level of connectivity, and stepping-stone dispersal over 64 generations predicted only one asymmetric barrier on the mid-Dutch coast (green barrier in Figure 1; Figure S2). Stepping-stone dispersal for the circadian behaviour showed a strong barrier on the south Jutland coast (purple barrier in Figure 1), and a few weaker, asymmetric barriers along the Dutch, Belgian and French coasts (Figure S2). The model of tidal vertical behaviour predicted three strong barriers (Figure S2) on the north Jutland coast, in the German Bight and on the mid-Dutch coast (turquoise barriers, Figure 1).

3.2 | Seascape genomic analyses

The first two axes of the PCA with all 24,273 loci showed 2.23% of the total inertia and distinguished three genetic clusters (Figure 2a). PC1 (1.26%) separates individuals sampled in the microtidal area of the Kattegat and Skagerrak (O, V and K), while PC2 (0.96%) shows differentiation between the individuals from the mesotidal sites of the North Sea, and the macrotidal sites from Bangor and Dunkirk (B and D). BAYESCAN identified 500 putative outlier loci at $q = 0.5$ and 128 outlier loci at $q = 0.00011$ (see Figure S1). These putative outlier loci represent 2% and 0.5% of all loci. Removing those outlier loci led to weaker differentiation among sites (Figure 2b), while the outlier loci also drew the same three distinct clusters (Figure 2c). Pairwise F_{ST} values among sites were low, ranging between 0 and 0.02 based on all loci (see Figure S3) and between 0 and 0.009 for neutral loci. In contrast, F_{ST} ranged between 0 and 0.363 for the 128 top outlier loci. F_{ST} was highest between the microtidal and the macrotidal cluster, which are also the most geographically distant sites. We did not find any differentiation related to sex (Figure S4).
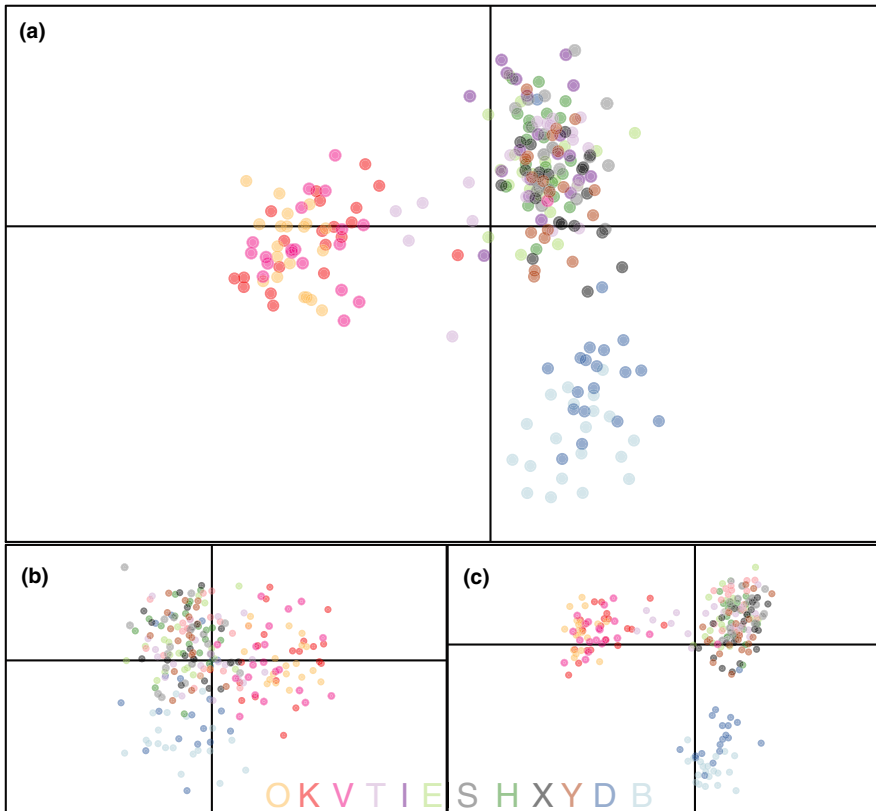
FIGURE 2 Principal component analyses for (a) all 24,273 loci (PC1: 1.26% inertia, PC2: 0.96% inertia), (b) all neutral loci, that is after removal of potential outlier loci identified in BAYESCAN with very relaxed $q = 0.5$ ($n = 500$; PC1: 0.84% inertia, PC2: 0.8% inertia), and (c) the 128 putative outlier loci identified in BAYESCAN with $q = 0.00011$ (PC1: 14.59% inertia, PC2: 10.84% inertia). Site acronyms and coloration as in Figure 1
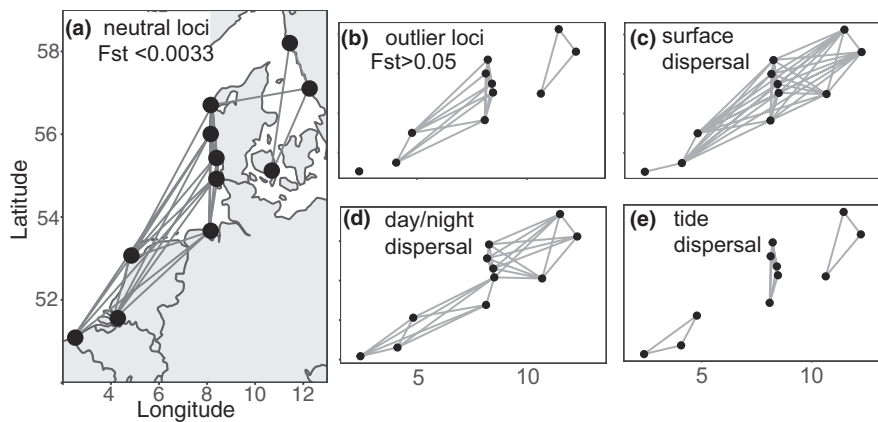
FIGURE 3 Networks of genetic distance (based on F_{ST} [a and b]) and oceanographic distance (based on dispersal probability from the biophysical model over 64 generations [c–e]) constructed for 11 sampling sites (Bangor was not included as it falls out of the oceanographic model domain) of *Carcinus maenas* in the North Sea. Lines indicate connectivity in terms of gene flow (a and b) and dispersal probability (c–e) and nodes (dots) are shown at their geographical location

IBD between F_{ST} and sea distance was significant for all data sets (all loci: $r^2 = 0.81$, neutral loci: $r^2 = 0.76$ and outlier loci: $r^2 = 0.82$, all $p < 0.0001$). There was no significant relationship between F_{ST} and multi(64)-generational dispersal probability from the biophysical modelling for any of the three behaviours. The network analyses based on F_{ST} were in line with the PCAs, showing no clear patterns of population structure for neutral loci, but three clusters for outlier loci (Figure 3a,b). The networks for the biophysical dispersal probabilities among the sampling sites showed large differences in connectivity estimates among the three dispersal behaviours with no

clear structure for the surface drifting larvae, but three clusters for larvae with tidal behaviour (Figure 3c–e).

The genetic cline analysis of the 128 outlier loci identified barriers to gene flow with obvious clustering of loci with steeper allelic clines at two geographical locations: ~1000 km (between the geographically close sites of Dunkirk and Yerseke) and 1700 km (separating the Skagerrak from the North Sea) from Bangor (Figure 4). These two barriers to gene flow closely reflect the separation into micro-, meso- and macrotidal areas (Figure 1). An LDna analysis (Kemppainen et al., 2015) did not indicate the presence of genomic

islands nor did it indicate that the loci at the tidal breaks shown in Figure 4 are in linkage disequilibrium (Figure S5). The number of markers showing evidence of clear allele frequency clines was higher along the transition from meso- to microtidal (15 loci with slope >0.002) than from macro- to mesotidal (four loci). Interestingly, demographic inferences suggested that different demographic histories were involved during the formation of the two barriers (Table 2 and Figure 5). Inferences performed between the meso- vs. microtidal sites showed relatively strong support for a secondary contact (SC) model including an expansion in the ancestral population and heterogeneous effective size across the genome (SC_ac_2N, with W_{AIC} =0.97, Table 2). The estimated contact period (~14 thousand years ago in the best model) was six times shorter than the isolation period (estimated to be 96,000 years, Table 2). In contrast, the SC model (including a recent expansion and heterogeneous effective population size across the genome, SC_rc_2N) and the isolation with migration (IM) model (including both ancient and recent expansion and heterogeneous effective population size or migration rate along the genome, IM_ac_rc_2N and IM_ac_rc_2 M) had a similar support for the meso- vs. macrotidal sites ($\Delta_{AIC} < 2$ for the three best models, Table 2). However, the parameter estimated for the SC model in the meso- vs. microtidal comparison were biologically unexpected (long divergence time >1 million years or isolation phase 50 times shorter than the secondary contact). Thus, an IM model is more likely to explain the divergence between the meso- vs. macrotidal site (Figure 5a). The two IM models differ only in the way genomic heterogeneity is captured and estimated similar parameter values (Table S1).

In our BLAST search of the 36-bp fragments of all 128 putative outlier loci, we only encountered 10 matches on the *Carcinus maenas*

TSA database, and blasting these longer contigs resulted in 41 *blastn* hits (Table S5). The hits were for five crustacean species and for a parasitic barnacle of the European shore crab (*Sacculina carcini*). Only a few predicted genes, all from *Homerus americanus*, were encountered. This is perhaps not surprising, as there are few genome references for crustaceans. One of these genes was mucin-3A-like, a glycoprotein component of a variety of mucus gels in humans, which may also be involved in ligand binding and intracellular signalling (UniProt). Other annotated outlier genes include the transposable element-derived protein 4-like piggyBac, a WD repeat-containing protein 19-like, and most interestingly two sterol O-acyltransferase 1-like transcripts. This acyl-transferase is also called ACAT1, and is one of the candidate genes we tested below, as differential expression of this genes has been shown in *Cellana rota* in a circa-tidal manner. The potential function of interest may be gravity impact (Casey et al., 2015; Frigeri et al., 2008; Schnytzer et al., 2018). However, the primer pair designed to amplify *C. maenas acat1* did not bind to any of the 10 TSA outlier sequences.

3.3 | Gene expression of putative clock genes

We were able to identify—for the first time in *C. maenas*—the orthologues of most clock components known from *Drosophila* as well as from other crustaceans. We identified and verified 21 orthologues of clock-related proteins, corresponding to insect core clock, clock-associated and clock input proteins (see Table S2). We found an "ancestral clock" in *C. maenas* with both *cry1* and *cry2* present in the transcriptome and expressed in crabs at all locations and in both megalopae and adults.
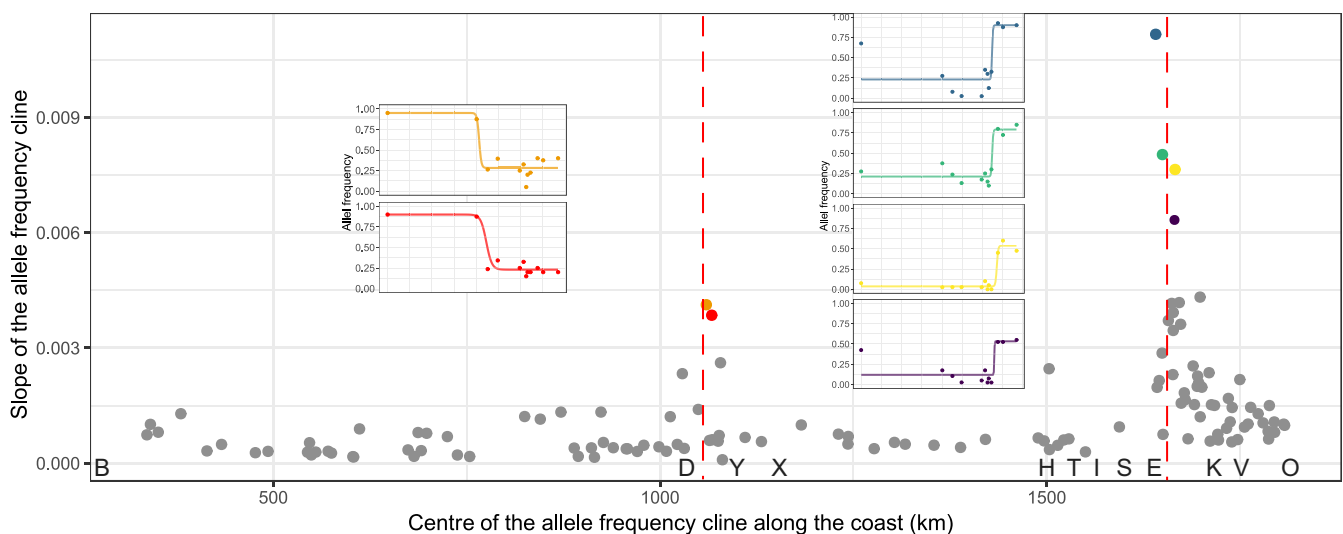
FIGURE 4 Geography of the genetic clines based on the slopes and centres of the allele frequencies of the 128 putative outlier loci as a function of sea distance from the site Bangor (B), the site with the highest tidal range. The dashed lines indicate the identified two barriers that separate macrotidal sites (B and D), mesotidal sites (Y, X, H, T, I, S, E) and the microtidal sites in the Kattegat/Skagerrak (K, V, O). Geographical locations of the sampling sites are approximate. Site acronyms are as in Figure 1. The inset panels show the clines of the loci with the strongest slopes at both barriers over the same geographical distance as shown in the main panel. The colour of the clines indicates the respective slope of the outlier locus in the same colour

TABLE 2 Summary of the demographic inferences showing the three best demographic histories inferred between populations from macro- vs. meso-, and meso- vs. microtidal sites

Data set	Model	likeli.	AIC	Δ_{AIC}	W_{AIC}	P	TS	TSC
Macro vs. Meso	SC_rc_2N	−591	1201	0	0.480	0.23	232	10,864
Macro vs. Meso	IM_ac_rc_2N	−591	1202	1	0.177	0.29	108	—
Macro vs. Meso	IM_ac_rc_2m	−590	1202	1	0.177	0.16	116	—
Meso vs. Micro	SC_ac_2N	−617	1255	0	0.973	0.34	95	16
Meso vs. Micro	IM_ac_rc_2N	−619	1259	4	0.018	0.36	123	—
Meso vs. Micro	SC_ac_rc_2N	−619	1260	5	0.007	0.25	83	14

Note: The table shows, in order of appearance, the population pairs, the best model (IM = isolation with migration, SC = secondary contact, rc and ac = recent and ancient change in effective size, 2N = heterogeneous effective size along the genome, 2m = heterogeneous migration rate along the genome); the AIC of the model, the difference of AIC with the best model (Δ_{AIC}), the weighted AIC (W_{AIC}), the proportion of the genome affected by low migration rate or low effective size (*P*), the time of split (T_s), and the time of secondary contact (T_{sc}) given in thousands of years. Other parameters estimated by the models are available in Table S1.
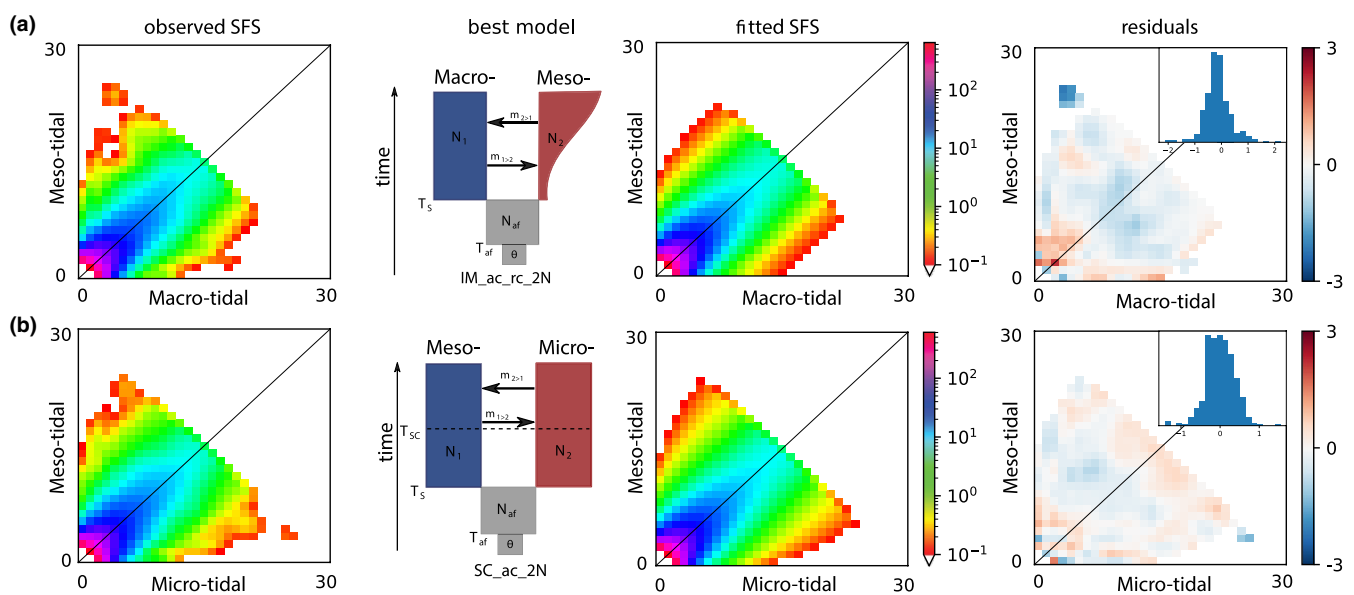
FIGURE 5 Result from the most likely scenario associated with the population divergence between (a) the macro- vs. mesotidal environment, and (b) meso- vs. microtidal environment. The graphs on each rows show the observed SFS, the schematic representation of the best demographic scenario (IM_ac_rc_2N: isolation with migration with change in effective size in ancestral and derived populations and with heterogeneous effective size along the genome; SC_ac_2N: secondary contact with change in effective size in the ancestral population and heterogeneous effective size along the genome), the fitted SFS and the residual of the model (containing the distribution of the residuals)

After Benjamini–Hochberg corrections, four out of the 21 candidate genes were significantly up- or down-regulated in at least one pairwise comparison of the six assessed sites (see Table S6). The linear model revealed a significant effect of the tidal gradient on gene expression of two genes: *pdp1* and *cyc* (Table S7). Both genes were generally down-regulated with increasing tidal amplitude and their patterns are very similar (Figure 6).

Other genes were significantly affected by the sampling date expressed in days after equinox (used as the reference, as at this date all sites experienced 12 h of daylight), and sampling time of the day (Table S7). The experiment was not designed to test for seasonal and daily expression patterns, but we have accounted for them in our linear model, and the identified genes may be interesting for

further investigations into the circadian clocks in *C. maenas*. In a data-reduction approach based on PCAs, tidal gradient had significant effects on expression of the core clock genes comprising *tim*, *cyc*, *clk*, *cry2* and *per* (Table S8, Figure S6).

4 | DISCUSSION

We set out with the hypothesis that tidal regime is a strong selection force on shore crab population structure, mostly driven by the fact that shore crab larvae show different vertical migration behaviours depending on the tidal amplitude. Vertical migration of *Carcinus maenas* larvae occurs with an endogenous tidal rhythm in tidal areas, and
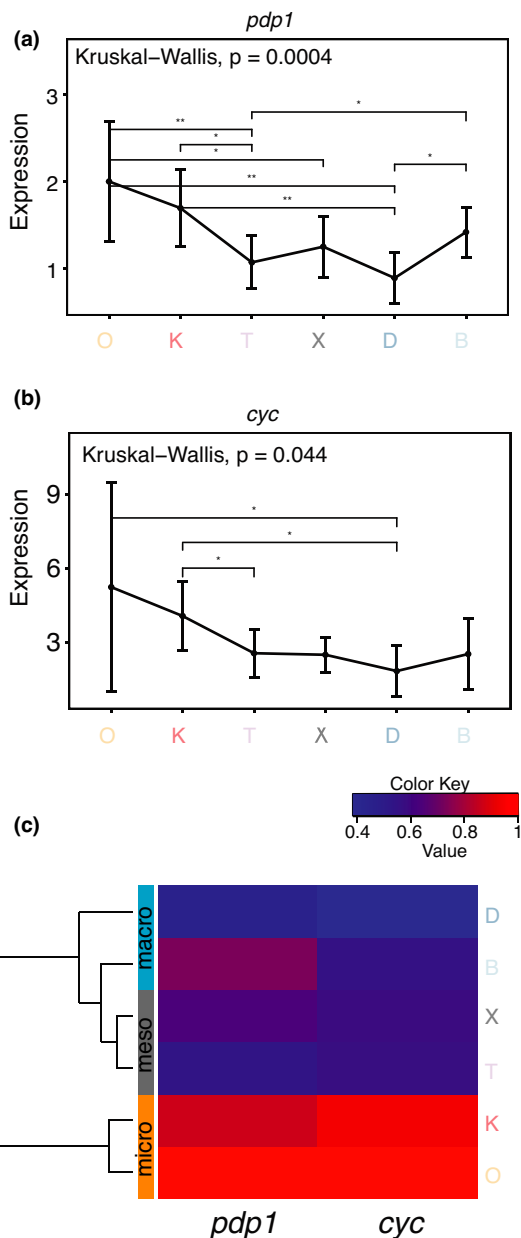
FIGURE 6 Effect of tidal amplitude on gene expression. Relative gene expression (normalized relative quantity [NRQ], standardized to individual D7F, a female from Dunkirk with generally low gene expression of many candidate genes) of genes significantly affected by the tidal gradient for (a) *pdp1* and (b) *cyc* along the tidal gradient from microtidal to large tidal amplitudes, and (c) heatmap of relative gene expression (NRQ, standardized to microtidal population from Odense) for both genes at all sites, assigned to their micro-, meso- or macrotidal location. Red indicates high expression. D, Dunkirk; B, Bangor; X, Texel; T, Thyborøn; K, Kristineberg; O, Odense

an exogenous circadian rhythm in microtidal areas (Moksnes et al., 2014; Queiroga et al., 2002). This tidal rhythm is heritable (Zeng & Naylor, 1996b), and we hypothesize that it may be regulated by clock genes, which are well described in insects and have also been found in some crustaceans (Biscontin et al., 2017; Christie et al., 2018). This behaviour has an impact on dispersal potential because according to the selective tidal stream transport hypothesis, vertical migration

between layers of opposite current directions is thought to facilitate cross-shelf transport and increase return of larvae to shallow nursery habitats (Duchêne & Queiroga, 2001; Zeng & Naylor, 1996a). Thus, "wrong" tidal behaviour may reduce recruitment success and thereby restrict dispersal between areas with different tidal regimes.

In our study we were able to show with oceanographic modelling of multigeneration, stepping-stone dispersal that larval vertical migration had a large effect on predicted long-term connectivity in the assessed geographical area. We found barriers to dispersal for all three modelled behaviours, with a barrier in the eastern Wadden Sea for both tidal and circadian behaviour, and with an additional barrier for tidal migration in the western Wadden Sea and at the border between the North Sea and Skagerrak (Figure 1).

Similar to previous population genetic assessments of the European and Mediterranean shore crab (Pascoal et al., 2009; Schiavina et al., 2014) we found weak F_{ST} ($F_{ST} = 0$–0.009 for neutral loci). Despite little population structure after removing 500 putative outliers (2% of all loci), we were able to detect a signal of IBD, suggesting that local recruitment patterns contribute to genetic differentiation in neutral loci. However, we did not find significant isolation-by-oceanography (IBO) based on multiple generation (64) dispersal probability for any modelled behaviour. Instead, the biophysical modelling indicates several strong barriers to dispersal (Figure 3) rather than a linear gradient in connectivity.

Using all ~24,000 SNPs and the 128 outlier loci, the shore crab samples clustered into three distinct groups (Figure 2a,c), driven by allele frequency clines at multiple loci whose centres are clustered at two localities (Figure 4). This suggests the presence of two main barriers to gene flow. These barriers spatially coincide with shifts in tidal regime (macro- vs. meso- vs. microtidal), but the two barriers seem to be shaped by different demographic histories (Figure 5). The barrier between micro- and mesotidal sites (i.e., between the Skagerrak and North Sea) seems to be a secondary contact zone between populations that have diverged in total isolation for about 90,000 years and then came in contact again (Table 2). The timing of secondary contact estimated here (14,000 years) approximately matches the ice retreat from the northern hemisphere (Hewitt, 2000), and is similar to the estimate obtained for the sand goby for secondary contact between North Sea and Baltic Sea populations (Leder et al., 2021).

A previous study exploring the genetic diversity of mitochondrial DNA in *C. maenas* described a genetic clade found only in populations from northern Europe, which could suggest the presence of a northern glacial refugium for the species (Roman & Palumbi, 2004). While it is not possible to infer the exact locations where isolation took place, one possibility to explain the secondary contact observed between the meso- and microtidal environment could involve a dual colonization of the North Sea – Baltic Sea system. Indeed, this area was mostly covered by land during the last glacial maximum, and was only accessible to marine life after the last deglaciation (about 15,000 years ago). Therefore, this secondary contact could correspond to the meeting point of two colonization waves, one coming from a northern refugium, and the other coming from the south, through the English Channel, as already previously suggested

for this species (Marino et al., 2011). These contact zones are expected to be stabilized at environmental or physical barriers to gene flow through coupling effects (Barton, 1979; Bierne et al., 2011). In agreement with the coupling hypothesis, our biophysical dispersal modelling suggests a strong oceanographic dispersal barrier for larvae with tidal migration behaviour at the transition zone between meso- and microtidal environment (Figures 1 and 3e). Interestingly, the alleles of some loci which showed a sharp frequency cline at the transition zone to the microtidal environment were also found at high frequency in Bangor (e.g., locus in blue and purple in the inset to Figure 4).

In contrast, our biophysical modelling does not suggest an oceanographic barrier spatially coinciding with the other genetic break present in the English Channel (i.e., the transition between meso- and macrotidal). Demographic modelling suggested isolation with migration over ~100,000 years at this genetic barrier, which is in line with previous estimates of ~470,000 years for the European ancestors of the two introduced lineages now found on the east coast of the USA (Jeffery, DiBacco, Wringe, et al., 2017). Altogether, the absence of complete historical isolation and the lack of an oceanographic barrier suggests that adaptation, and notably adaptation to tidal environments, contributes to the genetic differences observed between macro- and mesotidal sites. While our data suggest that tidal amplitude plays a major role in both barriers, other environmental drivers could also contribute. Temperature has been shown to play an important role in shaping population differentiation in several crustaceans, such as in American lobster (Benestan et al., 2016) and northern shrimp (Jorde et al., 2015), and a genomic island has been identified in the shore crab which might be associated with rapid temperature adaptation (Tepolt et al., 2021; Tepolt & Palumbi, 2020). The geographical area assessed here is located in the middle of the native distribution of *C. maenas*, which makes it less likely that physical factors such as temperature and salinity play a major role in shaping population genetic structure. Indeed, we do not find any evidence that salinity seems to drive the observed population structure of *C. maenas*, despite a strong salinity gradient from the North Sea going into the Skagerrak and Kattegat (see Figure S7). In the North West Atlantic, one barrier to connectivity has been described in Nova Scotia at a temperature gradient for multiple species, including *C. maenas* (Jeffery, DiBacco, & Wyngaarden, 2017; Stanley et al., 2018). However, their identified multispecies barrier also coincides with a tidal regime shift from macro- to mesotidal (Flemming, 2012), and we here argue for the importance of differences in recruitment success in larvae adapted to different tidal regimes, affecting dispersal, rather than temperature as also suggested by Pringle et al. (2011).

Finally, the detected differences in gene expression for two clock genes—probably involved in regulating circadian behaviour of crab larvae—could be part of the explanation for the maintenance of the two identified barriers to gene flow associated with tidal regime. Based on the data obtained here, it appears that shore crabs possess a circadian clock that relies on many of the same molecular components as other, better understood, invertebrate circadian clocks.

While the clock machinery for circadian rhythms is relatively well known (e.g., Crane & Young, 2014), little is known about which genes may be involved in tidal rhythms. The few studies investigating both circadian and lunar cycles (either for 12.4-h or 29-day periods) indicate that the two systems work independently and that lunar-related rhythms may not be generated by the canonical circadian clock genes (Bulla et al., 2017). Our results here confirm that circadian genes and putative tidal cyclers occur in transcriptomes of *C. maenas*, and that they are expressed in both adult and megalopae phases. With linear models, we identified two genes, the core clock gene *cyc* and the clock-associated gene *pdp1*, that may help explain behavioural differences among crab larvae from microtidal and tidal sites (macro- and mesotidal). In *Drosophila* constant high or low PDP1 levels disrupt locomotor activity rhythms, and although its function as a circadian oscillator is unknown, this suggests that PDP1 regulates oscillator output (Benito et al., 2007). This hypothesis is supported by our data, which showed that crabs that experience tides and do not follow a circadian rhythm (but a tidal rhythm) have a lower level of *pdp1* transcripts. Additionally, *acat1* may be a promising candidate gene for tidal cycling, as it was previously detected as a candidate "tidal cycler" in *Cellana rota*, and was among our few annotated outlier loci. However, we could only detect a weak effect of tidal gradient on gene expression of *acat1* (Table S4).

A driving question for our research was to investigate the proximal causes for the adaptation of differences in timing of vertical migration of crab larvae according to tidal regime. Overall, the line of evidence in this study is a large step towards understanding the contribution of behaviour to local adaptation. While this study is an integrativeassessment of different approaches, there are nevertheless gaps in our line of evidence that make conclusions uncertain. For the gene expression analysis, we are able to show a correlation of gene expression with tidal gradient for two candidate clock genes, but we are not able to determine if the difference is driven by a plastic response or if it is heritable, for instance due to allelic differences. Moreover, we infer patterns of expression of clock genes in larval stages from analyses of adult crabs. However, we show that the clock genes are also expressed in megalopae, and while sensing and reacting to changes in light and tide may be particularly relevant in crab larvae, both light and tide have also been shown to alter behaviour and activity in adult shore crabs (Naylor, 1958; Queiroga et al., 1994; Zeng & Naylor, 1997). In the future, the availability of a *C. maenas* reference genome and using larger genomic coverage, combined with experimental work establishing the direct link between different larval behaviours and gene expression over time (particularly circadian and circa-tidal), hold exiting potential to more fully understand the role of larval behaviour on the population structure of shore crabs. In particular, such assessments would help to conclude with more certainty that there are indeed locally adapted larval behaviours in *C. maenas* along a tidal gradient, which are mediated by genetic differences in clock gene alleles or their regulation. Additionally, such work could establish whether the identified clock genes (*pdp1* and *cyc*) do indeed directly or indirectly control larval behaviour.

Finally, selection for larval behaviour that increases return to near-coast habitats may explain regional differences and local adaptations of behaviour synchronized to regional hydrodynamic transport (Moksnes et al., 2014). In line with the perspective in Burgess et al. (2016), the pelagic larval stage may not only increase life-long fitness through access to food and reduced predation in the water column, but also be under selection for increased dispersal. Indeed, larval behaviours (e.g., synchronized with the tide) promote return to adult habitats, which may also reduce along-shore dispersal, and facilitate the evolution of locally adapted larval behaviours.

CONFLICT OF INTERESTS

The authors declare no conflict of interest.

AUTHOR CONTRIBUTIONS

P.R.J., P.O.M. and M.J. designed the research and performed the sampling. A.L.M. performed the demographic modelling, G.A.M. carried out the gene expression experiments, M.J. performed the bioinformatic and population genetic analyses and P.R.J. performed the biophysical modelling. M.J. led the writing of the paper, and all authors contributed to the writing process.

DATA AVAILABILITY STATEMENT

The 2bRAD raw sequences (fastq) are openly available on NCBI's sequence read archive (SRA) (BioProject PRJNA797386, accession nos.: SAMN25002278–SAMN25002565). Key downstream data files, such as the final filtered vcf files for all, neutral and outlier loci, and key new scripts for population genetics and dispersal analyses can be found at: 10.17044/scilifelab.17836025. The scripts for the 2b-RAD bioinformatic analysis are available at: https://github.com/z0on/2bRAD_denovo; and scripts for demographic inferences are available at: https://github.com/alanlm-speciation/moments_optimization.

ORCID

Marlene Jahnke https://orcid.org/0000-0001-7262-315X

REFERENCES

Abuhagr, A. M., Blindert, J. L., Nimitkul, S., Zander, Ian A., Labere, Stefan M., Chang, Sharon A., Maclea, Kyle S., Chang, Ernest S., & Mykles, Donald L. (2014). Molt regulation in green and red color morphs of the crab *Carcinus maenas*: gene expression of molt-inhibiting hormone signaling components. *Journal of Experimental Biology*, 217, 796–808.

Alexander, J. L., Oliphant, A., Wilcockson, D. C., Audsley, N., Down, R. E., Lafont, R., & Webster, S. G. (2018). Functional characterization and signaling systems of corazonin and red pigment concentrating hormone in the green shore crab, *Carcinus maenas*. *Frontiers in Neuroscience*, 11, 752. https://doi.org/10.3389/fnins.2017.00752

Barth, J. M. I., Villegas-Ríos, D., Freitas, C., Moland, E., Star, B., André, C., Knutsen, H., Bradbury, I., Dierking, J., Petereit, C., Righton, D., Metcalfe, J., Jakobsen, K. S., Olsen, E. M., & Jentoft, S. (2019). Disentangling structural genomic and behavioural barriers in a sea of connectivity. *Molecular Ecology*, 28, 1394–1411. https://doi.org/10.1111/mec.15010

Barton, N. (1979). Gene flow past a cline. *Heredity*, 43, 333–339. https://doi.org/10.1038/hdy.1979.86

Bates, D., Eigen, C., & Rcpp, L. (2014). Package 'lme4'. https://cran.r-project.org/web/packages/lme4/index.html.

Benestan, L., Quinn, B. K., Maaroufi, H. et al (2016). Seascape genomics provides evidence for thermal adaptation and current-mediated population structure in American lobster (*Homarus americanus*). *Molecular Ecology*, 25, 5073–5092.

Benito, J., Zheng, H., & Hardin, P. E. (2007). PDP1ε functions downstream of the circadian oscillator to mediate behavioral rhythms. *Journal of Neuroscience*, 27, 2539–2547.

Benjamini, Y., & Hochberg, Y. (1995). Controlling the false discovery rate: a practical and powerful approach to multiple testing. *Journal of the Royal Statistical Society: Series B (Methodological)*, 57, 289–300.

Bierne, N., Welch, J., Loire, E., Bonhomme, F., & David, P. (2011). The coupling hypothesis: why genome scans may fail to map local adaptation genes. *Molecular Ecology*, 20, 2044–2072. https://doi.org/10.1111/j.1365-294X.2011.05080.x

Biscontin, A., Wallach, T., Sales, G., Grudziecki, A., Janke, L., Sartori, E., Bertolucci, C., Mazzotta, G., De Pittà, C., Meyer, B., Kramer, A., & Costa, R. (2017). Functional characterization of the circadian clock in the Antarctic krill, *Euphausia superba*. *Scientific Reports*, 7, 17742. https://doi.org/10.1038/s41598-017-18009-2

Bjornstad, O. (2009). *ncf: spatial nonparametric covariance functions*. R package version 1.1-3. http://onb.Ent.Psu.Edu/onb1/r

Bonhomme, F., & Planes, S. (2000). Some evolutionary arguments about what maintains the pelagic interval in reef fishes. *Environmental Biology of Fishes*, 59, 365–383. https://doi.org/10.1023/A:1026508715631

Breteler-Klein, W. (1976). Settlement, growth and production of the shore crab, *Carcinus maenas*, on tidal flats in the Dutch Wadden Sea. *Netherlands Journal of Sea Research*, 10, 354–376. https://doi.org/10.1016/0077-7579(76)90011-9

Bulla, M., Oudman, T., Bijleveld, A. I., Piersma, T., & Kyriacou, C. P. (2017). Marine biorhythms: bridging chronobiology and ecology. *Philosophical Transactions of the Royal Society B: Biological Sciences*, 372, 20160253. https://doi.org/10.1098/rstb.2016.0253

Burgess, S. C., Baskett, M. L., Grosberg, R. K., Morgan, S. G., & Strathmann, R. R. (2016). When is dispersal for dispersal? Unifying marine and terrestrial perspectives. *Biological Reviews*, 91, 867–882. https://doi.org/10.1111/brv.12198

Casey, T., Patel, O. V., & Plaut, K. (2015). Transcriptomes reveal alterations in gravity impact circadian clocks and activate

mechanotransduction pathways with adaptation through epigenetic change. *Physiological Genomics*, 47, 113–128. https://doi.org/10.1152/physiolgenomics.00117.2014

Cayuela, H., Rougemont, Q., Laporte, M., Mérot, C., Normandeau, E., Dorant, Y., Tørresen, O. K., Hoff, S. N. K., Jentoft, S., Sirois, P., Castonguay, M., Jansen, T., Praebel, K., Clément, M., & Bernatchez, L. (2020). Shared ancestral polymorphisms and chromosomal rearrangements as potential drivers of local adaptation in a marine fish. *Molecular Ecology*, 29, 2379–2398. https://doi.org/10.1111/mec.15499

Christie, A. E., Yu, A., & Pascual, M. G. (2018). Circadian signaling in the Northern krill *Meganyctiphanes norvegica*: In silico prediction of the protein components of a putative clock system using a publicly accessible transcriptome. *Marine Genomics*, 37, 97–113. https://doi.org/10.1016/j.margen.2017.09.001

Corell, H., Moksnes, P.-O., Engqvist, A., Döös, K., & Jonsson, P. R. (2012). Depth distribution of larvae critically affects their dispersal and the efficiency of marine protected areas. *Marine Ecology Progress Series*, 467, 29–46. https://doi.org/10.3354/meps09963

Crane, B. R., & Young, M. W. (2014). Interactive features of proteins composing eukaryotic circadian clocks. *Annual Review of Biochemistry*, 83, 191–219. https://doi.org/10.1146/annurev-biochem-060713-035644

Crothers, J. (1967). The biology of the shore crab *Carcinus maenas* (L.) 1. The background-anatomy, growth and life history. *Field Studies*, 2, 407–434.

Csardi, G., & Nepusz, T. (2006). The igraph software package for complex network research. *InterJournal, Complex Systems*, 1695, 1–9.

Danecek, P., Auton, A., Abecasis, G., Albers, C. A., Banks, E., DePristo, M. A., Handsaker, R. E., Lunter, G., Marth, G. T., Sherry, S. T., McVean, G., & Durbin, R. (2011). The variant call format and VCFtools. *Bioinformatics*, 27, 2156–2158. https://doi.org/10.1093/bioinformatics/btr330

Darling, J. A., Tsai, Y.-H.- E., Blakeslee, A. M., & Roman, J. (2014). Are genes faster than crabs? Mitochondrial introgression exceeds larval dispersal during population expansion of the invasive crab Carcinus maenas. *Royal Society Open Science*, 1, 140202.

Dawirs, R. R. (1985). Temperature and larval development of *Carcinus maenas* (Decapoda) in the laboratory: Predictions of larval dynamics in the sea. *Marine Ecology Progress Series*, 24, 297–302. https://doi.org/10.3354/meps024297

Derryberry, E. P., Derryberry, G. E., Maley, J. M., & Brumfield, R. T. (2014). HZAR: hybrid zone analysis using an R software package. *Molecular Ecology Resources*, 14, 652–663.

Duchêne, J.-C., & Queiroga, H. (2001). Use of an intelligent CCD camera for the study of endogenous vertical migration rhythms in first zoeae of the crab *Carcinus maenas*. *Marine Biology*, 139, 901–909. https://doi.org/10.1007/s002270100633

Dyer, R. (2014). *Popgraph: This is an R package that constructs and manipulates population graphs*. R Package Version 1.4.

Edelaar, P., & Bolnick, D. I. (2012). Non-random gene flow: an underappreciated force in evolution and ecology. *Trends in Ecology & Evolution*, 27, 659–665. https://doi.org/10.1016/j.tree.2012.07.009

Flemming, B. W. (2012). Siliciclastic back-barrier tidal flats. In *Principles of tidal sedimentology* (pp. 231–267). Springer.

Foll, M. (2012). BayeScan v2. 1 user manual. *Ecology*, 20, 1450–1462.

Frigeri, A., Iacobas, D. A., Iacobas, S., Nicchia, G. P., Desaphy, J. F., Camerino, D. C., Svelto, M., & Spray, D. C. (2008). Effect of microgravity on gene expression in mouse brain. *Experimental Brain Research*, 191, 289–300. https://doi.org/10.1007/s00221-008-1523-5

Grosholz, E. D., & Ruiz, G. M. (1996). Predicting the impact of introduced marine species: lessons from the multiple invasions of the European green crab *Carcinus maenas*. *Biological Conservation*, 78, 59–66. https://doi.org/10.1016/0006-3207(94)00018-2

Hellemans, J., Mortier, G., De Paepe, A., Speleman, F., & Vandesompele, J. (2007). qBase relative quantification framework and software for management and automated analysis of real-time quantitative PCR data. *Genome Biology*, 8(2), 1–14.

Hewitt, G. (2000). The genetic legacy of the Quaternary ice ages. *Nature*, 405, 907–913. https://doi.org/10.1038/35016000

Hill, A. (1995). The kinematical principles governing horizontal transport induced by vertical migration in tidal flows. *Journal of the Marine Biological Association of the United Kingdom*, 75, 3–13. https://doi.org/10.1017/S0025315400015150

Ho, W.-C., & Zhang, J. (2018). Evolutionary adaptations to new environments generally reverse plastic phenotypic changes. *Nature Communications*, 9, 1–11.

Hordoir, R., Axell, L., Höglund, A., Dieterich, C., Fransner, F., Gröger, M., & Haapala, J. (2019). Nemo-Nordic 1.0: a NEMO-based ocean model for the Baltic and North seas–research and operational applications. *Geoscientific Model Development*, 12(1), 363–386.

Hurrell, J. W., & Deser, C. (2010). North Atlantic climate variability: the role of the North Atlantic Oscillation. *Journal of Marine Systems*, 79, 231–244. https://doi.org/10.1016/j.jmarsys.2009.11.002

Jahnke, M., Jonsson, P. R., Moksnes, P. O., Loo, Lars-Ove, Jacobi, Martin Nilsson, & Olsen, Jeanine L. (2018). Seascape genetics and biophysical connectivity modelling support conservation of the seagrass Zostera marina in the Skagerrak-Kattegat region of the eastern North Sea. *Evolutionary Applications*, 11, 645–661.

Jänicke, L., Ebener, A., Dangendorf, S., Arns, Arne, Schindelegger, Michael, Niehüser, Sebastian, Haigh, Ivan D., Woodworth, Philip L., & Jensen, Jürgen (2020). Assessment of tidal range changes in the North Sea from 1958 to 2014. *Journal of Geophysical Research: Oceans*, 126, e2020JC016456.

Jeffery, N. W., DiBacco, C., Van Wyngaarden, M., Hamilton, Lorraine C., Stanley, Ryan R. E., Bernier, Renée, Jennifer FitzGerald, K., Matheson, C. H., McKenzie, Praveen Nadukkalam, Ravindran, Robert Beiko, & Bradbury, Ian R. (2017). RAD sequencing reveals genomewide divergence between independent invasions of the European green crab (Carcinus maenas) in the Northwest Atlantic. *Ecology and Evolution*, 7, 2513–2524.

Jeffery, N. W., DiBacco, C., Wringe, B. F., Stanley, R. R. E., Hamilton, L. C., Ravindran, P. N., & Bradbury, I. R. (2017). Genomic evidence of hybridization between two independent invasions of European green crab (Carcinus maenas) in the Northwest Atlantic. *Heredity*, 119, 154–165. https://doi.org/10.1038/hdy.2017.22

Jombart, T. (2008). adegenet: a R package for the multivariate analysis of genetic markers. *Bioinformatics*, 24, 1403–1405. https://doi.org/10.1093/bioinformatics/btn129

Jonsson, P. R., Moksnes, P. O., Corell, H., Bonsdorff, E., & Nilsson Jacobi, M. (2020). Ecological coherence of Marine Protected Areas: New tools applied to the Baltic Sea network. *Aquatic Conservation: Marine and Freshwater Ecosystems*, 30, 743–760. https://doi.org/10.1002/aqc.3286

Jorde, P. E., Søvik, G., Westgaard, J. I., Albretsen, Jon, André, Carl, Hvingel, Carsten, Johansen, Torild, Sandvik, Anne, Kingsley, Michael C. S., & Jørstad, Knut Eirik (2015). Genetically distinct populations of northern shrimp, Pandalus borealis, in the North Atlantic: adaptation to different temperatures as an isolation factor. *Molecular Ecology*, 24, 1742–1757.

Jouganous, J., Long, W., Ragsdale, A. P., & Gravel, S. (2017). Inferring the joint demographic history of multiple populations: beyond the diffusion approximation. *Genetics*, 206, 1549–1567. https://doi.org/10.1534/genetics.117.200493

Kawecki, T. J., & Ebert, D. (2004). Conceptual issues in local adaptation. *Ecology Letters*, 7, 1225–1241. https://doi.org/10.1111/j.1461-0248.2004.00684.x

Kemppainen, P., Knight, C. G., Sarma, D. K., Hlaing, T., Prakash, A., Maung Maung, Y. N., Somboon, P., Mahanta, J., & Walton, C. (2015). Linkage disequilibrium network analysis (LD na) gives a global view of chromosomal inversions, local adaptation and geographic

structure. *Molecular Ecology Resources*, *15*, 1031–1045. https://doi.org/10.1111/1755-0998.12369

Kenkel, C. D., & Matz, M. V. (2016). Gene expression plasticity as a mechanism of coral adaptation to a variable environment. *Nature Ecology & Evolution*, *1*, 1–6.

Kuznetsova, A., Brockhoff, P. B., & Christensen, R. H. B. (2017). lmerTest package: tests in linear mixed effects models. *Journal of Statistical Software*, *82*. https://cran.r-project.org/web/packages/lmerTest/lmerTest.pdf

Le Moan, A., Bekkevold, D., & Hemmer-Hansen, J. (2021). Evolution at two time frames: ancient structural variants involved in post-glacial divergence of the European plaice (*Pleuronectes platessa*). *Heredity*, *4*(126), 1–16.

Leder, E. H., André, C., Le Moan, A., Töpel, M., Blomberg, A., Havenhand, J. N., Lindström, K., Volckaert, F. A. M., Kvarnemo, C., Johannesson, K., & Svensson, O. (2021). Post-glacial establishment of locally adapted fish populations over a steep salinity gradient. *Journal of Evolutionary Biology*, *34*, 138–156. https://doi.org/10.1111/jeb.13668

Li, W., & Godzik, A. (2006). Cd-hit: a fast program for clustering and comparing large sets of protein or nucleotide sequences. *Bioinformatics*, *22*, 1658–1659. https://doi.org/10.1093/bioinformatics/btl158

Marino, I. A., Pujolar, J. M., & Zane, L. (2011). Reconciling deep calibration and demographic history: Bayesian inference of post glacial colonization patterns in *Carcinus aestuarii* (Nardo, 1847) and *C. maenas* (Linnaeus, 1758). *PLoS One*, *6*, e28567.

Marshall, D., Monro, K., Bode, M., Keough, M., & Swearer, S. (2010). Phenotype–environment mismatches reduce connectivity in the sea. *Ecology Letters*, *13*, 128–140.

McKenna, A., Hanna, M., Banks, E., Sivachenko, A., Cibulskis, K., Kernytsky, A., Garimella, K., Altshuler, D., Gabriel, S., Daly, M., & DePristo, M. A. (2010). The Genome Analysis Toolkit: a MapReduce framework for analyzing next-generation DNA sequencing data. *Genome Research*, *20*, 1297–1303. https://doi.org/10.1101/gr.107524.110

Mohamedeen, H., & Hartnoll, R. (1989). Larval and postlarval growth of individually reared specimens of the common shore crab *Carcinus maenas* (L.). *Journal of Experimental Marine Biology and Ecology*, *134*, 1–24. https://doi.org/10.1016/0022-0981(90)90053-F

Moksnes, P.-O. (1999). Recruitment regulation in juvenile shore crabs *Carcinus maenas*: importance of intraspecific interactions in space limited refuge habitats. PhD thesis, Gothenburg University.

Moksnes, P.-O., Corell, H., Tryman, K., Hordoir, R., & Jonsson, P. R. (2014). Larval behavior and dispersal mechanisms in shore crab larvae (*Carcinus maenas*): Local adaptations to different tidal environments? *Limnology and Oceanography*, *59*, 588–602.

Moksnes, P.-O., Hedvall, O., & Reinwald, T. (2003). Settlement behavior in shore crabs *Carcinus maenas*: why do postlarvae emigrate from nursery habitats? *Marine Ecology Progress Series*, *250*, 215–230. https://doi.org/10.3354/meps250215

Momigliano, P., Florin, A.-B., & Merilä, J. (2021). Biases in demographic modelling affect our understanding of recent divergence. *bioRxiv*, 2020.006. 2003.128298.

Munday, P. L., Warner, R. R., Monro, K., Pandolfi, J. M., & Marshall, D. J. (2013). Predicting evolutionary responses to climate change in the sea. *Ecology Letters*, *16*, 1488–1500. https://doi.org/10.1111/ele.12185

Naylor, E. (1958). Tidal and diurnal rhythms of locomotory activity in *Carcinus maenas* (L.). *Journal of Experimental Biology*, *35*, 602–610.

Nosil, P. (2009). Adaptive population divergence in cryptic color-pattern following a reduction in gene flow. *Evolution*, *63*, 1902–1912. https://doi.org/10.1111/j.1558-5646.2009.00671.x

Pante, E., & Simon-Bouhet, B. (2013). Marmap: a package for importing, plotting and analyzing bathymetric and topographic data in R. *PLoS One*, *8*, e73051. https://doi.org/10.1371/journal.pone.0073051

Pascoal, S., Creer, S., Taylor, M. I., Queiroga, H., Carvalho, G., & Mendo, S. (2009). Development and application of microsatellites in *Carcinus maenas*: Genetic differentiation between northern and central Portuguese populations. *PLoS One*, *4*, e7268. https://doi.org/10.1371/journal.pone.0007268

Pfaffl, M. W., Horgan, G. W., & Dempfle, L. (2002). Relative expression software tool (REST©) for group-wise comparison and statistical analysis of relative expression results in real-time PCR. *Nucleic Acids Research*, *30*, e36.

Pickering, T. R., Poirier, L. A., Barrett, T. J., McKenna, S., Davidson, J., & Quijón, P. A. (2017). Non-indigenous predators threaten ecosystem engineers: interactive effects of green crab and oyster size on American oyster mortality. *Marine Environmental Research*, *127*, 24–31. https://doi.org/10.1016/j.marenvres.2017.03.002

Portik, D. M., Leaché, A. D., Rivera, D., Barej, M. F., Burger, M., Hirschfeld, M., Rödel, M.-O., Blackburn, D. C., & Fujita, M. K. (2017). Evaluating mechanisms of diversification in a Guineo-Congolian tropical forest frog using demographic model selection. *Molecular Ecology*, *26*, 5245–5263. https://doi.org/10.1111/mec.14266

Pringle, J. M., Blakeslee, A. M., Byers, J. E., & Roman, J. (2011). Asymmetric dispersal allows an upstream region to control population structure throughout a species' range. *Proceedings of the National Academy of Sciences*, *108*, 15288–15293. https://doi.org/10.1073/pnas.1100473108

Queiroga, H. (1998). Vertical migration and selective tidal stream transport in the megalopa of the crab *Carcinus maenas*. *Hydrobiologia*, *375*, 137–149.

Queiroga, H., Costlow, J. D., & Moreira, M. H. (1994). Larval abundance patterns of *Carcinus maenas* (*Decapoda, Brachyura*) in Canal de Mira. *Marine Ecology Progress Series*, *111*, 63–72.

Queiroga, H., Moksnes, P.-O., & Meireles, S. (2002). Vertical migration behaviour in the larvae of the shore crab *Carcinus maenas* from a microtidal system (Gullmarsfjord, Sweden). *Marine Ecology Progress Series*, *237*, 195–207. https://doi.org/10.3354/meps237195

Ravinet, M., Faria, R., Butlin, R. K., Galindo, J., Bierne, N., Rafajlović, M., Noor, M. A. F., Mehlig, B., & Westram, A. M. (2017). Interpreting the genomic landscape of speciation: a road map for finding barriers to gene flow. *Journal of Evolutionary Biology*, *30*, 1450–1477. https://doi.org/10.1111/jeb.13047

Richardson, J. L., Urban, M. C., Bolnick, D. I., & Skelly, D. K. (2014). Microgeographic adaptation and the spatial scale of evolution. *Trends in Ecology & Evolution*, *29*, 165–176. https://doi.org/10.1016/j.tree.2014.01.002

Riginos, C., Crandall, E. D., Liggins, L., Bongaerts, P., & Treml, E. A. (2016). Navigating the currents of seascape genomics: how spatial analyses can augment population genomic studies. *Current Zoology*, *62*, 581–601. https://doi.org/10.1093/cz/zow067

Roman, J. (2006). Diluting the founder effect: cryptic invasions expand a marine invader's range. *Proceedings of the Royal Society B: Biological Sciences*, *273*, 2453–2459. https://doi.org/10.1098/rspb.2006.3597

Roman, J., & Palumbi, S. R. (2004). A global invader at home: population structure of the green crab, *Carcinus maenas*, in Europe. *Molecular Ecology*, *13*, 2891–2898. https://doi.org/10.1111/j.1365-294X.2004.02255.x

Rougemont, Q., Gagnaire, P. A., Perrier, C., Genthon, Clémence, Besnard, Anne-Laure, Launey, Sophie, & Evanno, Guillaume (2017). Inferring the demographic history underlying parallel genomic divergence among pairs of parasitic and nonparasitic lamprey ecotypes. *Molecular Ecology*, *26*, 142–162.

Rougeux, C., Bernatchez, L., & Gagnaire, P.-A. (2017). Modeling the multiple facets of speciation-with-gene-flow toward inferring the divergence history of lake whitefish species pairs (*Coregonus clupeaformis*). *Genome Biology and Evolution*, *9*, 2057–2074. https://doi.org/10.1093/gbe/evx150

Sanford, E., & Kelly, M. W. (2011). Local adaptation in marine invertebrates. *Annual Review of Marine Science*, 3, 509–535. https://doi.org/10.1146/annurev-marine-120709-142756

Savolainen, O., Lascoux, M., & Merilä, J. (2013). Ecological genomics of local adaptation. *Nature Reviews Genetics*, 14, 807. https://doi.org/10.1038/nrg3522

Schiavina, M., Marino, I., Zane, L., & Melià, P. (2014). Matching oceanography and genetics at the basin scale. Seascape connectivity of the Mediterranean shore crab in the Adriatic Sea. *Molecular Ecology*, 23, 5496–5507. https://doi.org/10.1111/mec.12956

Schnytzer, Y., Simon-Blecher, N., Li, J., Waldman Ben-Asher, H., Salmon-Divon, M., Achituv, Y., Hughes, M. E., & Levy, O. (2018). Tidal and diel orchestration of behaviour and gene expression in an intertidal mollusc. *Scientific Reports*, 8, 4917. https://doi.org/10.1038/s41598-018-23167-y

Shanks, A. L. (1995). Mechanisms of cross-shelf dispersal of larval invertebrates and fish. In L. R. McEdward (Eds.), *Ecology of marine invertebrate larvae* (pp. 324–367). CRC.

Sjöqvist, C., Godhe, A., Jonsson, P., Sundqvist, L., & Kremp, A. (2015). Local adaptation and oceanographic connectivity patterns explain genetic differentiation of a marine diatom across the North Sea-Baltic Sea salinity gradient. *Molecular Ecology*, 24, 2871–2885. https://doi.org/10.1111/mec.13208

Stanley, R. R. E., DiBacco, C., Lowen, B., Beiko, R. G., Jeffery, N. W., Van Wyngaarden, M., Bentzen, P., Brickman, D., Benestan, L., Bernatchez, L., Johnson, C., Snelgrove, P. V. R., Wang, Z., Wringe, B. F., & Bradbury, I. R. (2018). A climate-associated multispecies cryptic cline in the northwest Atlantic. *Science Advances*, 4, eaaq0929. https://doi.org/10.1126/sciadv.aaq0929

Tepolt, C., Grosholz, E., de Rivera, C. E., & Ruiz, G. (2021). Balanced polymorphism fuels rapid selection in an invasive crab despite high gene flow and low genetic diversity. *Molecular Ecology*, 31(1), 55–69. https://doi.org/10.1111/mec.16143

Tepolt, C. K., & Palumbi, S. R. (2015). Transcriptome sequencing reveals both neutral and adaptive genome dynamics in a marine invader. *Molecular Ecology*, 24, 4145–4158. https://doi.org/10.1111/mec.13294

Tepolt, C. K., & Palumbi, S. R. (2020). Rapid adaptation to temperature via a potential genomic island of divergence in the invasive green crab, *Carcinus maenas*. *Frontiers in Ecology and Evolution*, 8, 411.

Vries, P., & Döös, K. (2001). Calculating Lagrangian trajectories using time-dependent velocity fields. *Journal of Atmospheric and Oceanic Technology*, 18(6), 1092–1101.

Wang, S., Meyer, E., McKay, J. K., & Matz, M. V. (2012). 2b-RAD: a simple and flexible method for genome-wide genotyping. *Nature Methods*, 9, 808–810. https://doi.org/10.1038/nmeth.2023

Warnes, G. R., Bolker, B., Bonebakker, L., Gentleman, R., Huber, W., Liaw, A., Lumley, T., Mächler, Martin, Magnusson, Arni, & Möller, Steffen (2009). *gplots: Various R programming tools for plotting data*. R package version 2, 1.

White, C., Selkoe, K. A., Watson, J., Siegel, D. A., Zacherl, D. C., & Toonen, R. J. (2010). Ocean currents help explain population genetic structure. *Proceedings of the Royal Society B: Biological Sciences*, 277, 1685–1694. https://doi.org/10.1098/rspb.2009.2214

Wickham, H. (2016). *ggplot2: elegant graphics for data analysis*. Springer.

Yamada, S. B., Peterson, W. T., & Kosro, P. M. (2015). Biological and physical ocean indicators predict the success of an invasive crab, *Carcinus maenas*, in the northern California Current. *Marine Ecology Progress Series*, 537, 175–189. https://doi.org/10.3354/meps11431

Zeng, C., & Naylor, E. (1996a). Endogenous tidal rhythms of vertical migration in field collected zoea-1 larvae of the shore crab *Carcinus maenas*: implications for ebb tide offshore dispersal. *Marine Ecology Progress Series*, 132, 71–82. https://doi.org/10.3354/meps132071

Zeng, C., & Naylor, E. (1996b). Heritability of circatidal vertical migration rhythms in zoea larvae of the crab *Carcinus maenas* (L.). *Journal of Experimental Marine Biology and Ecology*, 202, 239–257. https://doi.org/10.1016/0022-0981(96)00023-8

Zeng, C., & Naylor, E. (1996c). Synchronization of endogenous tidal vertical migration rhythms in laboratory-hatched larvae of the crab *Carcinus maenas*. *Journal of Experimental Marine Biology and Ecology*, 198, 269–289. https://doi.org/10.1016/0022-0981(96)00004-4

Zeng, C., & Naylor, E. (1997). Rhythms of larval release in the shore crab *Carcinus maenas* (Decapoda: Brachyura). *Journal of the Marine Biological Association of the United Kingdom*, 77, 451–461.

SUPPORTING INFORMATION

Additional supporting information may be found in the online version of the article at the publisher's website.